

# Effect of Temperature Photo Degradation of Titanium Dioxide Doped with Mg for Antibacterial Application

Seenaa Wdaah Man Allh Al-Salih

The General Directorate of Education, Dhi Qar Governorate, Iraq

---

**Received:** 2025, 15, Jul

**Accepted:** 2025, 21, Aug

**Published:** 2025, 15, Sep

Copyright © 2025 by author(s) and Scientific Research Publishing Inc. This work is licensed under the Creative Commons Attribution International License (CC BY 4.0).



Open Access

<http://creativecommons.org/licenses/by/4.0/>

**Annotation:** Using a sol-gel process, titanium dioxide doped with Mg nanoparticles was synthesized with a temperature modification. By reducing by catalytic agent preparation of Mg-doped TiO<sub>2</sub> for evaluation of the capacity antibacterial activity, bio-materials in nanopowder in solid-state produced interlocking among the anatase surface nanoparticles after that, they served as a capping and stabilizing agent. The Mg-doped TiO<sub>2</sub> NPs. XRD, SEM, and UV-vis methods were used to describe the samples. The temperature variation impacted the scale, shape, as well as the purity of Mg-doped TiO<sub>2</sub> NPs. According to XRD measurements, the average crystallite size dropped from 23.23nm to 20.70nm, while the energy band decreased from 3.33eV to 2.62eV based on UV-vis measurements. The antibacterial activity of Mg-doped TiO<sub>2</sub> NPs was investigated using growing minimum inhibitory concentration of gram-negative bacteria *E. coli* and *Klebsiella* spp, as well as gram-positive bacteria *S.aureus* and *S.epidermidis*, and the fungus *Candida albicans*. The zones for Mg-doped TiO<sub>2</sub> NPs were between (12-13) 37C° when 25C° was

---

between (11-12) mm. The zones for (Mg-doped TiO<sub>2</sub>) NPs were formed when the temperature of 40C° was between (12.5-14) mm. The findings of this investigation show that as the temperature rises, so does the ratio of degraded bacterial media.

**Keywords:** photo catalyst, anti-bacteria, Titanium Dioxide Doped with Mg, nanoparticles.

---

## 1-Introduction

The last decade has seen the start of a scientific revolution based on the ability to measure, manipulate and organize matter on a nanometric scale. Nanotechnology together with information technologies and biotechnology are fields that they have undergone dizzying developments in the last 15 years [1]. Nanotechnology and nanoscience are two areas of research already established that encompass discovery, understanding and application of new properties that emerge or are improved from the control of the composition, structure and size of the matter nano scale. Nobel Prize winner Richard Feynman, in 1959, he was the first to refer to the possibilities of nanoscience and nanotechnology in his famous speech entitled: There's Plenty of Room at the Bottom. Leftover) [2]. He predicted that a large number of new discoveries would be made if materials of atomic or molecular dimensions. With the advancement of techniques experiments and the development of Scanning Tunnel Microscopy (STM) or Atomic Force (AFM), at the end of the 80s it became. It is possible to observe materials at the atomic scale and the manipulation of individual atoms. Nanoscale control involves the ability to manufacture products and build machines with atomic precision. Manufacturing on a "nano" scale means being able to access and manipulate the molecular structures and their atoms. To give you an idea of the scale on which nanotechnology is developed: the head of apin measures between one and two millimeters (10T<sup>3</sup> m), the cells of the plants and animals reach between ten and one hundred microns (10T<sup>6</sup>m), a small molecule or the size of several aligned atoms equals at one nano meter (10T<sup>9</sup> m) (cf. figure 1). All the materials, devices, instruments, etc., that fall within this scale are consider (nanomaterials) or nano technological devices. The nanotechnology promises solutions to multiple problems that currently facing humanity, such as environmental, energy, health (nanomedicine), and many others Nanotechnology has gained in popularity and relevance in recent years [1]. Nanotechnology [2] is the study of the development, manipulation, and use of nanometer-scale materials.

Ecologically responsible nanomaterials manufacturing methods that do not include the use of toxic chemicals are becoming more significant [3]. Cost savings, environmental friendliness, and the absence of high pressure, energy, temperature, or hazardous substances are all advantages of sol-gel synthesis over chemical and physical synthesis techniques [4]. The plant extract is used as a reducing and capping agent in the production of green nanoparticles, eliminating the need for dangerous reducing chemicals. The particles are disseminated in the solvent in this situation.

A colloidal suspension, commonly known as a sol, is created. In the second step, due to the condensation of the sol, these colloidal particles can be bonded together, and they can still remain in the solvent to form an open 3D network termed a gel. Salt became jelly. When contrasted to others, it forms a gel-like protrusion. Solid state methods, plasma spraying, solution sedimentation, hydrothermal methods, and heat of fusion are only a few examples. Synthesis, for

example. [5-8] The advantages of using a sol-gel process are as follows:

In the application domain, there is a lot to offer. Because Gel Salt Catalysts always contain a variety of components. Components (active metal ions on an oxide substrate) or alloying (metallic or nonmetallic) introduction into the oxide [9-13]. TiO<sub>2</sub> nanoparticles are interesting candidates for solar energy applications due to their unique photoelectronics and optical capabilities. Photovoltaic performance for effective solar energy conversion radiation, in particular, TiO<sub>2</sub> nanoparticles garner a lot of attention. TiO<sub>2</sub>, particularly the anatase phase, has been highlighted for its potential applicability in the gaseous and liquid decomposition of numerous environmental toxins. In any case, it has a number of drawbacks. Large bandgap (3.2 V) that creates the majority of the solar energy spectrum that is not consumed. Various activators were added to TiO<sub>2</sub> to boost optical absorption in the visible region and hence increase its solar efficiency. [14-20]

## 1.2 Effect of Temperature

Because photocatalytic devices do not require heating and may function at room temperature, the apparent activation energy in the medium temperature range (20°C-80°C) is frequently quite low (a few kJ/mol). At very low temperatures (-40°C-0°C), however, activity decreases and activation energy increases [21]. The rate-limiting phase is often desorption. For many types of photocatalytic processes, however, at "high" temperatures (>70-80°C), activity falls and the reported threshold voltage goes negative. [22]

## 2. Experimental framework

In terms of being linked to an electrical outlet, solid materials are divided into three categories: conducting materials, insulation, and semi-conductor materials. As seen in figure, this categorization is based on the band gap and consequently the amount of energy gap fig. (1).

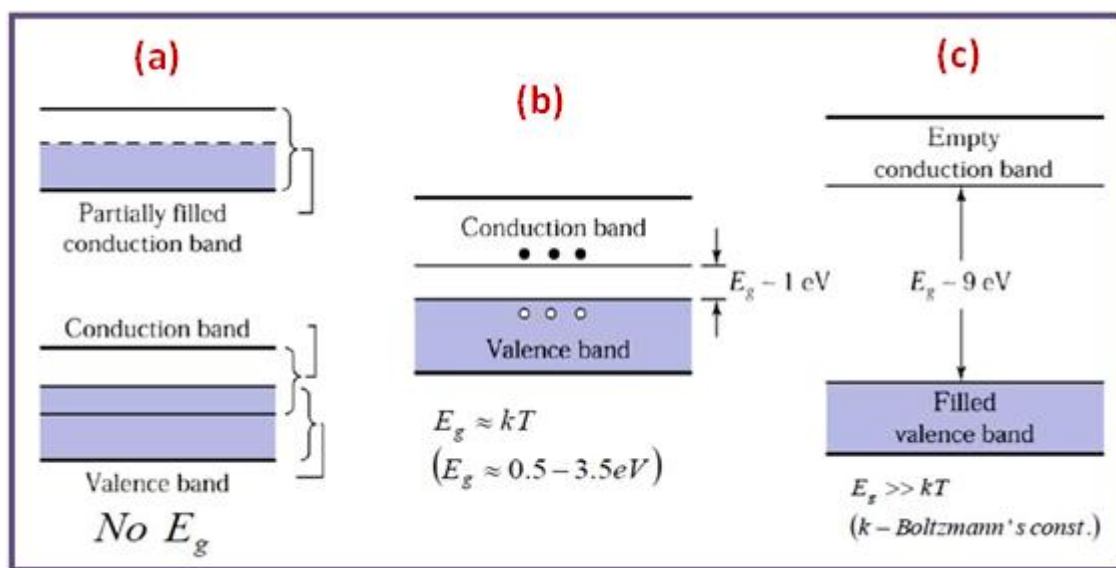


**Figure (1): Energy bands in solids: (a) conductor; (b) semiconductor; (c) insulator** <sup>(10)</sup>

A bandgap separates an almost filled valence band and a virtually empty conduction band in a semiconductor material like Mg-doped TiO<sub>2</sub>. The conduction band (CB) is totally devoid of electrons, whereas the valence band (VB) is completely populated with valence electrons. A valence band electron (e<sup>-</sup>) can be thermally stimulated into the (CB) at a limited temperature, leaving an unfilled state in the valence band (VB). A hole (h<sup>+</sup>) is an empty condition that may be thought of as a second carrier of positive charge.

### 2.1 Prepare of Mg-doped TiO<sub>2</sub> nanoparticles

The majority of the compounds utilized in the study are commonplace. In most cases, chemicals are readily available in the laboratory. V Titanium isopropoxide and magnesium nitrate were

employed in this experiment. Due to their electrical and chemical characteristics, metal oxide nanoparticles have recently received a lot of attention. Specifications. Mg and Mg-doped TiO<sub>2</sub> are discussed in this article. The catalytic activity of the nanoparticles was quite high. The sol-gel process was used to make it. The sol-gel method is a technique for separating solids from liquids.

Because they make it extremely easy to manipulate particle size and the experimental method, it is a flexible approach used to synthesis diverse oxides. According to Alsalih *et al.*, (2021), the nano powders of Mg-doped TiO<sub>2</sub> [23].

The adsorption measurement was achieved at dark for whole reaction with various pH values and different temperatures with period (2,5,7,10,15,20,30,60,90,120,150) min. Whole photo reactions with various pH values and different temperatures (controlled using water bath) was repeated at dark to investigate the adsorption of were measured according to the changing in solution concentrations of MB dye , at  $\lambda_{max}$  (664nm) by UV- visible spectrophotometry.

## 2.2 Antimicrobial activity of Mg-doped TiO<sub>2</sub> NPs

Four bacterial cultures were obtained from the Institute of Biological Sciences at the University of Putra, two of which are Gram-positive (*S.aureus*, *S.epidermidis*) and Gram-negative (*Escherichia coli*, *Klebsiella spp.*) In addition to culture media for fungi such as (*Candida albicans*). Where it was first tested through the osmotic activity of the experiment of osmosis of molecules through diffusion through the dinner of the ornament for each of them separately. Then the osmotic activity of the nanoparticles was tested in the solid-state photocatalyzed for the compound of titanium catalyzed by magnesium, the experiment was carried out in two stages, the first in normal sunlight with laboratory lighting The second is dark interactions to compare the effect of nanocomposites through testing the influencing factor and the antibacterial influencing concentration capable of ripping the walls and genetic material of the interstitium and critical inhibition of both antioxidant enzymes and bacterial repair systems through a sequence of temperature changes.[13].

25 mL of nutritional agar was placed into sterilized Petri plates with a 90 mm diameter for the test. To recover the strain, the plates were coated with a bacterial sample and incubated at 37 ° C for 24 hours. Under aseptic circumstances, the pure colony was chosen, transferred to nutrient broth, and cultivated for 24 hours at 37 degrees Celsius. Fresh agar plates were inoculated with broth cultures and 0.8 cm wells were created using diffusion plate procedures. 80 l of Mg-doped TiO<sub>2</sub> nanoparticles were put into two independent wells on a single plate. At 37 ° C, plates containing Mg-doped TiO<sub>2</sub> nanoparticles and the strains under investigation were incubated for 24 hours. On their outer surface, gram-negative bacteria contain an extra layer of lipopolysaccharides and peptidoglycans. Table 1, Figure 2, and Diagram are examples of this (1).

## Results and Discussion

**Table (1) Demonstrated inhibition zone results of Mg-doped TiO<sub>2</sub> nanoparticles.**

Type of bacteria	25°C	37°C	40°C
Staphylococcus aureus	11mm	12.5 m m	13.5 m m
Staphylococcus Epidermidis	12mm	12.2 m m	12.5 m m
E.coli	11.5mm	13.3 m m	13.5 m m
Klebseilla spp	11.4mm	12. m m	12.9 m m
Candida albicans	12m m	13. m m	14 mm

**Table 2. Demonstrated the statistical analysis of inhibition zone by the effect of NPs exposure**

Type of test	N	Mean	Std. Deviation	Std. Error Mean	Sig. (2-tailed)
test1	5	11.58	.426	.190	0.00
test2	5	12.60	.543	.242	0.00
test3	5	13.28	.584	.261	0.00
mean	3	12.48	.855	.494	.002

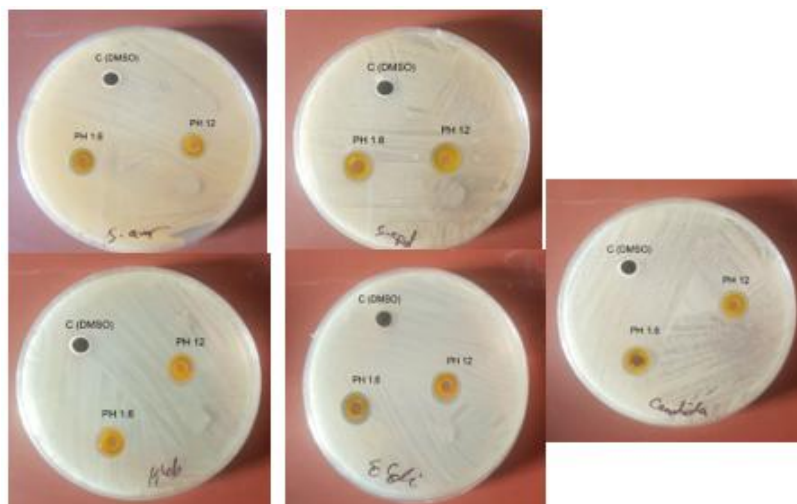


**Fig (2) Antimicrobial activity of TiO<sub>2</sub> doped with Mg**

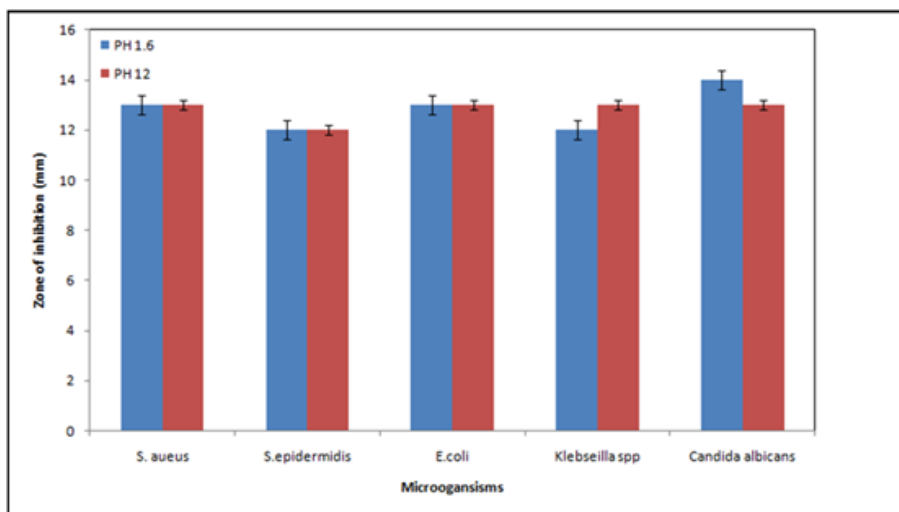


**Figure (3) Antimicrobial potency of biosynthesized**

Figures 2 and 3 shown the inhibition zone of the media, the results were summarized in table 1 and 2 where found high significant difference according the change of assay temperature. Photocatalytic reaction was studied by using UV-Vis spectrophotometry. In photocatalytic reaction the effect of the catalyst on photocatalytic rate of decomposition of growth of bacteria through the use of catalyst TiO<sub>2</sub> and TiO<sub>2</sub>- solid state reaction (Mg-doped TiO<sub>2</sub> (300,400)) and (Mg-doped TiO<sub>2</sub> (500 ,750 ) the results of prepare nanoparticles go with [20-24]. Using constant weight of the catalyst and different media. The most effective weight was found (1\*10<sup>-4</sup> M). At best weight the influence of many factors on rate of decomposition of growth of bacteria were studied the iThe effect of temperature variation from (25, 37, 40°C) and found that increased rate of decomposition with increasing the temperature of the media. Activation energy (Ea) for each reaction was calculated by using the equation of Arrhenius equation between (5.73–11.31) kJ mol<sup>-1</sup>.

A series of dark reactions with absorbance measurement by UV-Vis spectrophotometry, within different periods of time with the change of pH and temperature. The results indicate that no degradation of the growth of bacteria although all the factors affecting in the photocatalytic present except UV-light, the finding of inhibition of bacteria growth correspondence with [22,23]

**Effect of Temperature inhibition of bacterial growth**

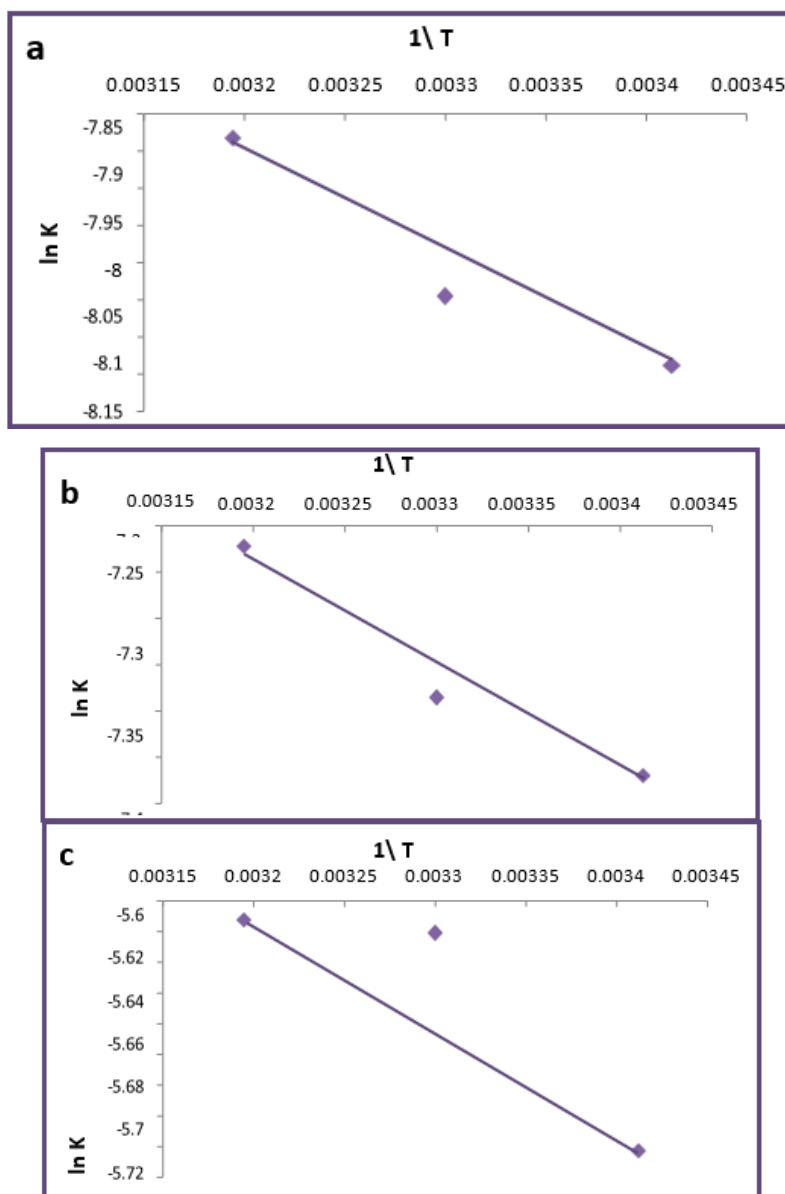
The ratio of decomposed media increasing the temperature. The activation energy parameters can be calculated from the plot of  $(lnk)$  versus  $(1/T)$  (Figure (4) and table 3, which gives the value of activation energy ( $E_a$ ) of each models of nanoparticles, according to the Arrhenius equation[24]:

$$lnk = lnA - \frac{E_a}{RT} \quad \text{..... (1)}$$

Where:  $E_a$  : Activation energy ( $kJmol^{-1}$ )  $A$  : Frequency factor ( $s^{-1}$ )

$R$ : Gas constant ( $0.008314 kJ K^{-1}mol^{-1}$ )  $T$ : Absolute temperature

Where the slope equals  $(-E_a/R)$  and the intercept equals  $(ln A)$ , shown in table (2) and figure (4). The adsorption of media was a physisorption process because the ( $E_a$ ) value as between  $(11.31 - 5.73) kJ k^{-1} mol^{-1}$



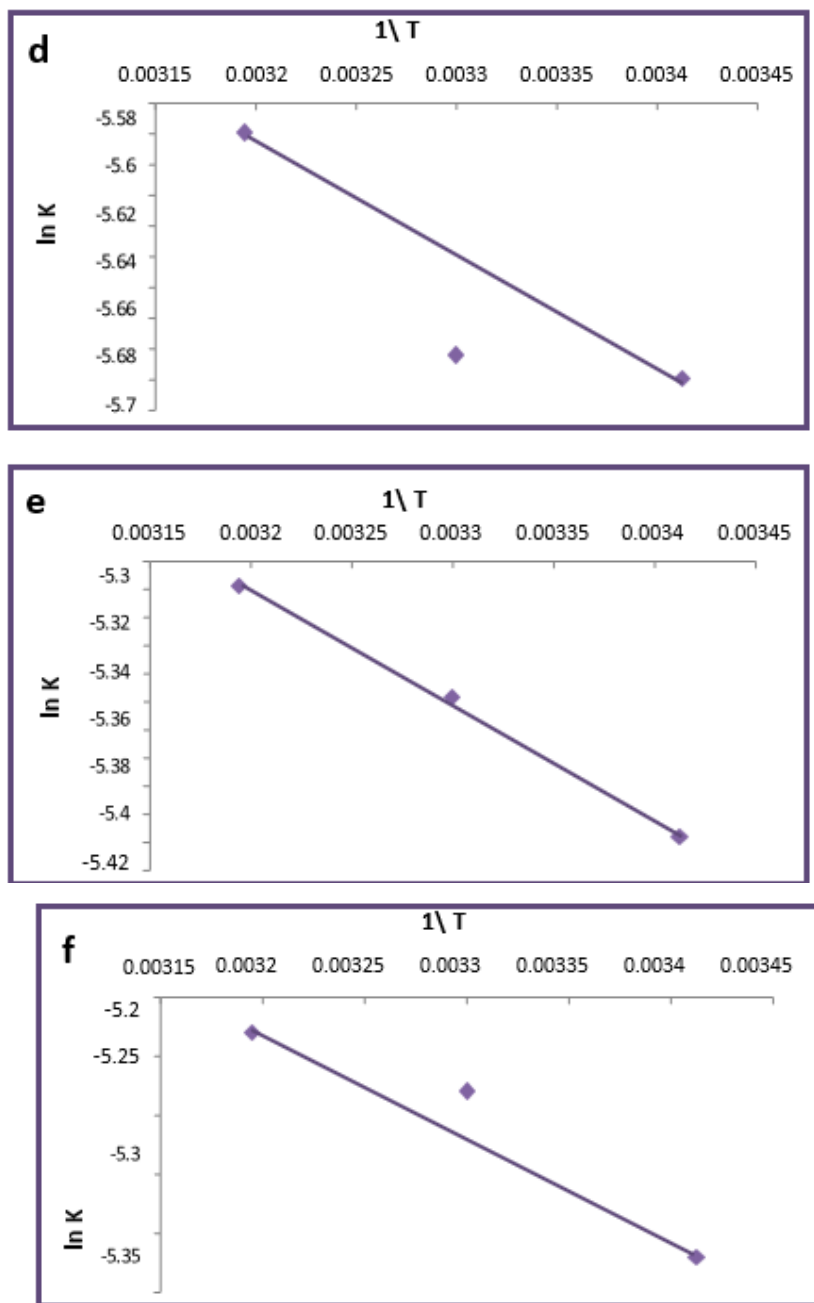


Figure (4): Plot of time vs.  $\ln k$  a- TiO<sub>2</sub> (Rutile) b- TiO<sub>2</sub> (Anatase) c- TiO<sub>2</sub>- Mg<sub>4</sub> (300 ) d- TiO<sub>2</sub>-Mg (400 ) e- TiO<sub>2</sub>-Mg (500 ) f- TiO<sub>2</sub> -Mg(750)

**Table (2): The rate constant and activation energy parameters for the photocatalytic inhibition of growth of bacteria and catalysis under UV light**

Sample No.	T (K)	1/T (K <sup>-1</sup> ) *10 <sup>-3</sup>	k (min <sup>-1</sup> ) *10 <sup>-3</sup>	- Ln k (min <sup>-1</sup> )	(kJmol <sup>-1</sup> )
TiO <sub>2</sub> (Anatase)	293	3.41	0.27	8.11	11.31
	303	3.30	0.30	8.09	
	313	3.19	0.37	7.81	
TiO <sub>2</sub> (Rutile)	293	3.41	0.57	7.66	13.51
	303	3.30	0.62	7.38	
	313	3.19	0.73	7.30	
	293	3.41	2.89	5.76	

<b>TiO<sub>2</sub>- Mg300</b>	<b>303</b>	<b>3.30</b>	<b>3.62</b>	<b>5.62</b>	<b>5.73</b>
	<b>313</b>	<b>3.19</b>	<b>3.65</b>	<b>5.61</b>	
<b>TiO<sub>2</sub>- Mg 400</b>	<b>293</b>	<b>3.41</b>	<b>3.15</b>	<b>5.76</b>	<b>6.13</b>
	<b>303</b>	<b>3.30</b>	<b>3.20</b>	<b>5.74</b>	
	<b>313</b>	<b>3.19</b>	<b>3.70</b>	<b>5.59</b>	
<b>TiO<sub>2</sub>- Mg 500</b>	<b>293</b>	<b>3.41</b>	<b>4.10</b>	<b>5.49</b>	<b>6.79</b>
	<b>303</b>	<b>3.30</b>	<b>4.53</b>	<b>5.39</b>	
	<b>313</b>	<b>3.19</b>	<b>4.90</b>	<b>5.31</b>	
<b>TiO<sub>2</sub>- Mg750</b>	<b>293</b>	<b>3.41</b>	<b>4.42</b>	<b>5.42</b>	<b>7.27</b>
	<b>303</b>	<b>3.30</b>	<b>5.09</b>	<b>5.28</b>	
	<b>313</b>	<b>3.19</b>	<b>5.35</b>	<b>5.23</b>	

## 1- Conclusion:

Inert titanium dioxide particles were used, which were saturated with magnesium ions to form a nano-decomposed powder in the manual case, a very simple chemical method, pulverizing at a temperature of 300 degrees Celsius for two hours, up to a temperature of 750 Kelvin, with a change in the reaction temperature with nanoparticles from 25 degrees Celsius to 45 degrees Celsius. The results of the examination of the microscope known as XRD showed that the size of the crystals changed from 23.23 nm to 20.70 nm with the increase in temperature in a controlled sequence. The size of the particles of the (TiO<sub>2</sub>-Mg) NPs was around 101.60 nm in the SEM pictures, but it fell to 34.30 nm when the temperature of the experimental conditions rose. The energy band grew from 3.33 to 5.62 eV, according to UV-visible measurements. The zones of growth inhibition of gram-negative bacteria *E. coli*, *Klebsiella* spp, and gram-positive bacteria *S. aureus*, *S. epidermidis*, and the fungus *Candida albicans* were used to investigate the antibacterial activity of TiO<sub>2</sub>-Mg NPs. When the temperature was 25 (11-12) mm, the zones for NPs (TiO<sub>2</sub>-Mg) were formed. When the temperature was 37°C, the zones for NPs (TiO<sub>2</sub>-Mg) were recorded.

## References

1. Fatimah, I., Green synthesis of silver nanoparticles using extract of *Parkia speciosa* Hassk pods assisted by microwave irradiation. *Journal of advanced research*, 2016. **7**(6): p. 961-969.
2. Kavitha, K., et al., Plants as green source towards synthesis of nanoparticles. *Int Res J Biol Sci*, 2013. **2**(6): p. 66-76.
3. Philip, D., Rapid green synthesis of spherical gold nanoparticles using *Mangifera indica* leaf. *Spectrochimica Acta Part A: Molecular and Biomolecular Spectroscopy*, 2010. **77**(4): p. 807-810.
4. VG, V.K. and A.A. Prem, Green synthesis and characterization of iron oxide nanoparticles using *Phyllanthus niruri* extract. *Oriental Journal of Chemistry*, 2018. **34**(5): p. 2583-2589.
5. Bhuiyan, M.S.H., et al., Green synthesis of iron oxide nanoparticle using *Carica papaya* leaf extract: application for photocatalytic degradation of remazol yellow RR dye and antibacterial activity. *Heliyon*, 2020. **6**(8): p. e04603.
6. Nagajyothi, P., et al., Green synthesis of iron oxide nanoparticles and their catalytic and in vitro anticancer activities. *Journal of Cluster Science*, 2017. **28**(1): p. 245-257.
7. Demirezen, D.A., et al., Green synthesis and characterization of iron oxide nanoparticles using *Ficus carica* (common fig) dried fruit extract. *Journal of bioscience and bioengineering*, 2019. **127**(2): p. 241-245.
8. Vujtek, M., et al., Ultrafine particles of iron (III) oxides by view of AFM–Novel route for study of polymorphism in nano-world. *Science, Technology and Education of Microscopy*, 2003. **1**(8): p. 1-8.

9. Kanagasubbulakshmi, S. and K. Kadirvelu, Green synthesis of iron oxide nanoparticles using *Lagenaria siceraria* and evaluation of its antimicrobial activity. *Defence Life Science Journal*, 2017. **2**(4): p. 422-427.
10. Salem, D.M., M.M. Ismail, and M.A. Aly-Eldeen, Biogenic synthesis and antimicrobial potency of iron oxide (Fe<sub>3</sub>O<sub>4</sub>) nanoparticles using algae harvested from the Mediterranean Sea, Egypt. *The Egyptian Journal of Aquatic Research*, 2019. **45**(3): p. 197-204.
11. Bouafia, A. and S.E. Laouini, Green synthesis of iron oxide nanoparticles by aqueous leaves extract of *Mentha Pulegium* L.: Effect of ferric chloride concentration on the type of product. *Materials Letters*, 2020. **265**: p. 127364.
12. Chauhan, S. and L.S.B. Upadhyay, Biosynthesis of iron oxide nanoparticles using plant derivatives of *Lawsonia inermis* (Henna) and its surface modification for biomedical application. *Nanotechnology for Environmental Engineering*, 2019. **4**(1): p. 8.
13. Vasantharaj, S., et al., Biosynthesis of iron oxide nanoparticles using leaf extract of *Ruellia tuberosa*: antimicrobial properties and their applications in photocatalytic degradation. *Journal of Photochemistry and Photobiology B: Biology*, 2019. **192**: p. 74-82.
14. Shibata S, Aoki K, Yano T, Yamane M. Preparation of silica microspheres containing Ag nanoparticles. *Journal of sol-gel science and Technology*. 1998 Aug;11(3):279-87.
15. Zhao Q, Yi L, Jiang L, Ma Y, Lin H, Dong J. Osteogenic activity and antibacterial ability on titanium surfaces modified with magnesium-doped titanium dioxide coating. *Nanomedicine*. 2019 Jan;14(9):1109-33.
16. Liu Y, Tian L, Tan X, Li X, Chen X. Synthesis, properties, and applications of black titanium dioxide nanomaterials. *Science Bulletin*. 2017 Mar 30;62(6):431-41.
17. Fang W, Xing M, Zhang J. A new approach to prepare Ti<sup>3+</sup> self-doped TiO<sub>2</sub> via NaBH<sub>4</sub> reduction and hydrochloric acid treatment. *Applied Catalysis B: Environmental*. 2014 Nov 1;160:240-6.
18. Şahin, Ö., İzgi, M.S., Onat, E. and Saka, C., 2016. Influence of the using of methanol instead of water in the preparation of Co–B–TiO<sub>2</sub> catalyst for hydrogen production by NaBH<sub>4</sub> hydrolysis and plasma treatment effect on the Co–B–TiO<sub>2</sub> catalyst. *International journal of hydrogen energy*, *41*(4), pp.2539-2546.
19. Prabu KM, Anbarasan PM. Preparation and Characterization of Silver, Magnesium & Bismuth Doped Titanium Dioxide Nanoparticles for Solar Cell Applications. *International Journal of Science and Research*. 2014;3:132-7.
20. Fernandez-Garcia M, Martinez-Arias A, Hanson JC, Rodriguez JA. Nanostructured oxides in chemistry: characterization and properties. *Chemical reviews*. 2004 Sep 8;104(9):4063-104.
21. Al-Salih M, Samsudin S, Rashid AR. Evaluation of cellular oxidative stress levels in aedes aegypti mosquitoes as a reaction of photo catalyst modify nanoparticles exposure. *Eurasian Journal of Biosciences*. 2020 Sep 26;14(2):3607-16.
22. Al-Salih M, Samsudin S, Arshad SS. Synthesis and characterizations iron oxide carbon nanotubes nanocomposite by laser ablation for anti-microbial applications. *Journal of Genetic Engineering and Biotechnology*. 2021 Dec;19(1):1-8.
23. AlSalih, M., Samsudin, S. and Arshad, S.S., 2021, August. Cellular Total Lipid Peroxidation, and Glutathione S Transferase Levels in Larvae and Pupae of *Aedes Aegypti* with Catalysts Preparation of Mg-doped tio<sub>2</sub> Nanoparticles. In *Journal of Physics: Conference Series* (Vol. 1973, No. 1, p. 012124). IOP Publishing.
24. Xing M, Li X, Zhang J. Synergistic effect on the visible light activity of Ti<sup>3+</sup> doped TiO<sub>2</sub> nanorods/boron doped graphene composite. *Scientific reports*. 2014 Jun 30;4(1):1-7.